

Evaluation of the frequency of the H-maser 1401701 by the primary frequency standard NPL-CsF1

National Physical Laboratory

February 2005

Summary

The primary frequency standard NPL-CsF1 was used to measure the frequency of the H-maser HM1 identified by the clock code 1401701 during three campaigns in 2004. These evaluations were performed by measuring mean frequency differences over the reporting periods. The frequency differences are given in table 1, together with the total uncertainty in relating NPL-CsF1 to maser1401701.

Period	MJD	$y(\text{CsF1}) - y(\text{HM1}) [\times 10^{-15}]$	$u(\text{total}) [\times 10^{-15}]$
I	53049 – 53084	0.5	1.2
II	53089 – 53119	3.5	1.2
III	53119 – 53149	7.2	1.2

Table 1. Summary of the frequency measurement of clock 1401701 (HM1) including the total uncertainty.

A brief description of the evaluation of the major systematic frequency biases, the measurement procedure, and a discussion of the uncertainties is presented in this report.

A detailed description of the measurement procedure together with a complete evaluation of the systematic frequency biases and their uncertainties is given in reference [1].

Systematic frequency biases

Those biases and uncertainties used to calculate the total contribution to the frequency of NPL-CsF1 (including the contribution from the gravity potential relative to the Earth's geoid) are listed in table 2:

Effect	Bias ($\times 10^{-15}$)	Uncertainty ($\times 10^{-15}$)
2 nd order Zeeman	142.7	0.1
AC Stark (BBR)	-16.9	0.4
Collisions	-7.7 ^{*)}	0.8
μ -w leakage	0.8	0.3
Cavity pulling	0.0	0.1
μ -w spectrum	0.0	<0.1
Cavity phase	0.0	0.3
Rabi, Ramsey pulling	0.0	0.1
AC Stark (lasers)	0.0	0.1
Gravity	1.3	0.1
Total (1σ), u_B		1.0

^{*)} The value of frequency bias due to cold collisions is given for example only. The actual value is computed continuously and standard's frequency is extrapolated to zero atomic density.

Table 2.

The evaluation of the major frequency biases is summarised below.

Second order Zeeman effect

A detailed map of the C-field applied in NPL-CsF1 was made before and after each evaluation period. This was done by recording Ramsey fringes on the "field sensitive" transition ($4,1 \leftrightarrow 3,1$) for incrementally increased launch height. The position of the central fringe for the operating launch height was verified periodically during the campaign.

The dominant contribution to the uncertainty of the second order Zeeman effect was the temporal instability of the C-field intensity. Peak-to-peak variations of less than 30 pT were observed over months of operation. For the average C-field value of 175 nT, the variations resulted in an uncertainty of the frequency bias of less than 1×10^{-16} .

AC Stark effect due to black-body radiation

The value of the black-body radiation frequency bias was obtained by monitoring the temperature of the NPL-CsF1 vacuum flight tube. Calibrated Pt100 sensors were used and the temperature values were logged by a computer every minute. To calculate the frequency bias the formula

$$\Delta\nu = \beta \left(\frac{T}{300} \right)^4 \left[1 + \varepsilon \left(\frac{T}{300} \right)^2 \right]$$

was used, with the coefficients β and ε taken from reference [2].

The peak-to-peak temporal variation in the temperature of the vacuum vessel was less than 0.1 K. However, the lower part of the flight tube was warmer, by nearly 2 K, than the upper part due to the heat dissipated by the MOT coils. Taking this value as an estimate of the temperature uncertainty, the uncertainty of the bias due to black-body radiation is 4×10^{-16} .

Collisions

To extrapolate the fountain frequency to the zero-density value, it was operated in an alternating mode, where every two cycles the density of the cold atomic sample was toggled between a high and low value. The following formula was used:

$$f_{zero} = \frac{f_{low} - r f_{high}}{1 - r}$$

where f_{zero} is the frequency extrapolated to the zero-density value and f_{low} and f_{high} are the measured frequencies for low and high atomic density respectively. The ratio r between the low and high density was approximately 1/2. The value used in the extrapolation formula was calculated from the amplitude of the detection signal measured and recorded every cycle.

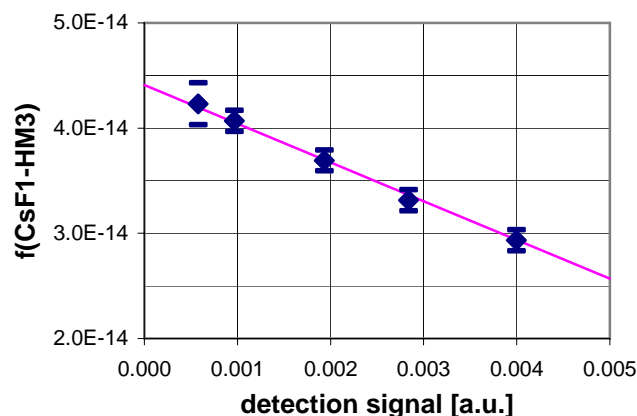


Fig. 1. The fractional frequency difference NPL-CsF1 – HM3 as a function of the detected atom number N_{at} . The maser frequency drift over the measurement time was removed. The straight line is a least squares fit to the experimental data.

In NPL-CsF1 the atomic density was not controlled directly, the detected fluorescence was controlled and hence the number of atoms N_{at} , reaching the detection zone. The linearity between N_{at} and the frequency bias was demonstrated, by measuring the

fractional frequency difference between NPL-CsF1 and one of the NPL hydrogen masers (fig.1). A type B uncertainty of 8×10^{-16} , associated with the extrapolation procedure, was calculated from the statistical uncertainty of the data collected for each value of N_{at} . Note, that the linear fit from fig. 1 was not used as a transfer function between the detection signal and the correction for the bias due to collisions; it was used solely to validate this extrapolation procedure. During a measurement campaign the fountain was operated exclusively in the alternating mode, correcting for the bias due to collisions.

Microwave leakage

The frequency of NPL-CsF1 was perturbed by the residual microwave field experienced by the atoms during the Ramsey time; the bias was linearly dependent on the microwave power. By changing the microwave field amplitude in the microwave cavity from $\pi/2$ to $11\pi/2$ (a power increase of a factor of 121), the bias was quantified with an uncertainty dominated by the stability of the bias. The level of the microwave leakage was verified regularly showing stability within 3×10^{-16} .

Gravity

The resonant frequency of atoms in the fountain was corrected for the gravity potential. The gravity potential was calculated from the height relative to the surface of constant gravity potential, the geoid (orthometric height). The orthometric height was obtained from survey data relative to the Ordinance Datum Newlyn (ODN) (whose position was known relative to the geoid). The uncertainty in the bias of the frequency relative to that of the SI second as realised on the geoid was estimated to be 1×10^{-16} due to an uncertainty of approximately 1 metre in the orthometric height for the laboratory where NPL-CsF1 is housed.

Measurement procedure

The frequency of NPL-CsF1 was related to a hydrogen maser HM3 (not reported to BIPM), which in turn was linked to the maser HM1. The two masers were located 0.8 km apart and an underground cable maintained a 10 MHz link between them.

During the measurement campaign the fountain was run exclusively in the alternating mode between high and low atom number. Additional noise due to the correction procedure and the link between HM1 and HM3 resulted in a short-term stability of the NPL-CsF1 – HM1 frequency difference of 7.5×10^{-13} in 1s (fig. 2).

Corrections due to effects other than collisions were sufficiently stable over the campaign period, so that a single correction value could be applied. Nevertheless, the validity of that value, where possible, was checked during a campaign. All the corrections were checked at the start and end of a campaign (e.g. a detailed map of the magnetic field was made). The temperature of the vacuum vessel was recorded at one-minute intervals. The microwave leakage level and the C-field value for the operating launch height (31 cm above the microwave cavity) were checked every two or three days.

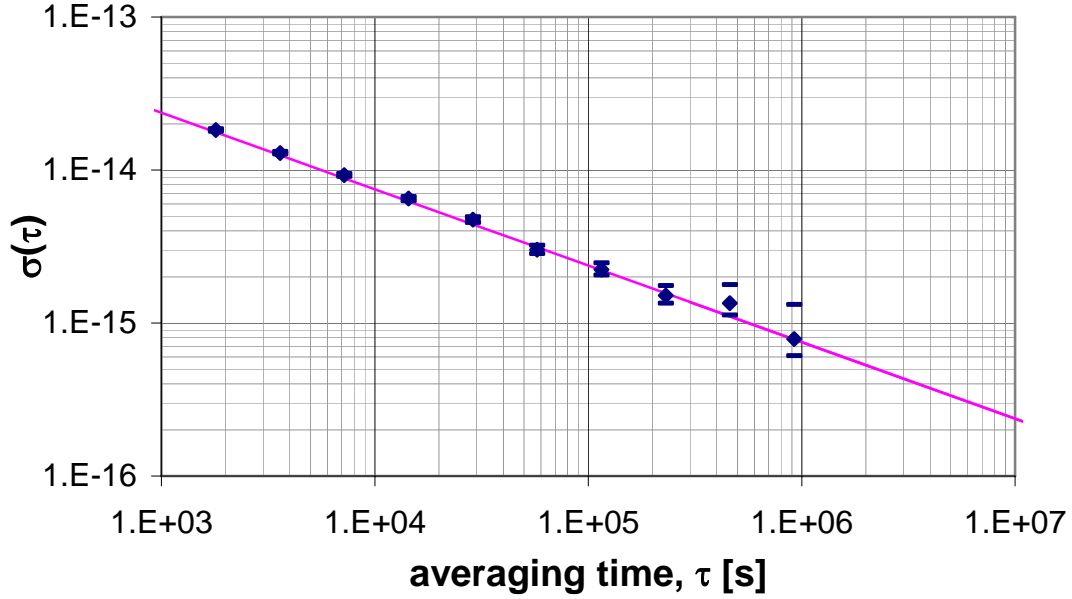


Fig. 2. Short-term stability of the CsF1–HM1 frequency difference extrapolated to zero atomic density. Linear frequency drift is removed (Hadamard deviation).

Uncertainties of the measurement

Stability

The short-term stability of the measurement of the frequency extrapolated to zero atomic density was typically 7.5×10^{-13} in 1s (7.5×10^{-15} in 10^4 s, see fig. 2). The type A uncertainty of the complete measurement u_A was obtained by assuming white FM noise over the effective period of integration (effective period = reporting period \times duty cycle).

Link with the local time scale

The uncertainty of the link with the local time scale $u_{l/lab}$ is a quadratic sum of two contributions:

$$(u_{l/lab})^2 = (u_{link})^2 + (u_{dt})^2$$

where u_{link} is the uncertainty associated with the frequency transfer between CsF1 and HM1 by the 0.8 km long 10 MHz link, and u_{dt} is an additional uncertainty of the measured maser frequency due to gaps (dead time) in the operation of the fountain standard.

In order to estimate the u_{link} , which arose predominantly from instabilities of the temperature of the linking cable, the round-trip phase-delay in the cable was monitored and the following value was ascribed to the uncertainty:

$$u_{link} = 0.4 \times 10^{-15}$$

Duty cycle (dead time)

During the evaluation period there were gaps in the data collection (dead time) due to both intentional and unintentional breaks. The intentional breaks were required to verify the C-field value and the microwave leakage level. Most of the unintentional breaks were caused by failures of the laser stabilisation system.

The uncertainty introduced by the dead time, u_{dt} , was approximated by calculating the time deviation (TDEV) of each gap, using the relation between TDEV and the modified Allan deviation (MDEV):

$$\sigma_x^2(\tau) = \tau^2/3 \text{ mod } \sigma_y^2(\tau),$$

where $\sigma_x(\tau)$ is the TDEV and $\text{mod } \sigma_y(\tau)$ is the MDEV.

The stability of the maser 1401701 has been shown to be dominated by flicker frequency modulation (ref. [3]) and the Hadamard deviation has been measured to be

$$\sigma_h(\tau) \cong 1.2 \times 10^{-15}; \quad 500 < \tau[\text{s}] < 6 \times 10^5.$$

The approximation, $\text{mod } \sigma_y(\tau) = \sigma_h(\tau)$, was used.

The fractional frequency uncertainty, u_{dt} , arising from the dead time was approximated by the square root of the sum of the time variances, normalised by the length of the measurement campaign, thus:

$$u_{dt} = \frac{1}{T} \sqrt{\sum_{i=1}^N [\sigma_x(\tau_i)]^2}$$

where $\sigma_x(\tau_i)$ is the time deviation (TDEV) of the maser over a duration τ_i ; and T is the duration of the campaign.

The longest dead time was 4 days. The uncertainty arising from the dead time for the campaigns was:

$$u_{dt}(\text{I}) = 1.4 \times 10^{-16}$$

$$u_{dt}(\text{II}) = 1.3 \times 10^{-16}$$

$$u_{dt}(\text{III}) = 2.0 \times 10^{-16}.$$

The uncertainty due to an uncorrected frequency drift of the maser 1401701 for the longest gap is known (ref. [3]) to be negligible when compared to the type A uncertainty of NPL-CsF1 over the same duration. The frequency drift of the maser was therefore omitted from the total uncertainty.

Evaluation results

Detailed parameters and results of the evaluation of the UTC(NPL) rate for the three periods in 2004 are listed in table 3. The total uncertainty u_{total} of the measurement is defined as:

$$(u_{total})^2 = (u_A)^2 + (u_B)^2 + (u_{l/lab})^2$$

Period		I	II	III
MJD		53049-53084	53089-53119	53119-53149
duration	days	35	30	30
duty cycle	%	57.4	70.7	81.8
$y(CsF1) - y(HM1)$	$\times 10^{-15}$	0.54	3.47	7.24
u_A	$\times 10^{-15}$	0.57	0.55	0.53
u_B	$\times 10^{-15}$	1.0	1.0	1.0
$u_{l/lab}$	$\times 10^{-15}$	0.42	0.42	0.45
u_{total}	$\times 10^{-15}$	1.2	1.2	1.2

Table 3.

References:

- [1] K. Szymaniec, W. Chalupczak, P.B. Whibberley, S.N. Lea, D. Henderson, *Metrologia*, **42**, (2005).
- [2] E. Simon, P. Laurent, A. Clairon. *Phys. Rev. A*, **57**, pp. 436-439, (1998).
- [3] J.A. Davis, C.A. Greenhall, P.W. Stacey, *Metrologia*, **42**, pp. 1-10, (2005)